Journal of Environmental Chemical Engineering 9 (2021) 106286

Contents lists available at ScienceDirect

Journal of Environmental Chemical Engineering

journal homepage: www.elsevier.com/locate/jece

Efficient nitrogen removal and recovery from real digested sewage sludge reject water through electroconcentration

Veera Koskue [a,b,*], Stefano Freguia [c], Pablo Ledezma [b], Marika Kokko [a]

[a] Faculty of Engineering and Natural Sciences, Tampere University, Korkeakoulunkatu 8, 33720 Tampere, Finland
[b] Advanced Water Management Centre, The University of Queensland, Gehrmann Laboratories Building (60), Brisbane, QLD 4072, Australia
[c] Department of Chemical Engineering, The University of Melbourne, Grattan Street, Parkville, VIC 3010, Australia

ARTICLE INFO

Editor: Dr. GL Dotto

Keywords:
Nutrient removal
Nutrient recovery
Nitrogen cycle
Centrate
Electrochemistry
Electroconcentration

ABSTRACT

Reject waters from the dewatering of anaerobically digested municipal sewage sludge are nitrogen-rich (ca. 1 $g_{NH4\text{-}N}$ L^{-1}) wastewater streams. They account for up to 25% of the total nitrogen load of wastewater treatment due to their internal recirculation within treatment plants. In this study, nitrogen was effectively removed and recovered from real reject water using a novel electrochemical setup combining electroconcentration and stripping. High nitrogen removal ($\leq$ 94 $\pm$ 0.7%) and recovery ($\leq$ 87 $\pm$ 8.5%) efficiencies from real reject water were obtained while simultaneously reducing the influent nitrogen concentration of 913 $\pm$ 14 $mg_{NH4\text{-}N}$ L^{-1} to 57 $\pm$ 6.7 $mg_{NH4\text{-}N}$ L^{-1} in the effluent. Most of the nitrogen recovery took place via electroconcentration into a liquid concentrate ($\leq$ 82 $\pm$ 5.7%), while stripping contributed little to the removal and recovery ($\leq$ 5 $\pm$ 2.8%). The reported removal and recovery efficiencies are the highest to date for a system utilising three-chamber electroconcentration. Furthermore, the concept of cation load ratio (the ratio between applied current density and cation loading rate) was introduced as a more precise parameter than the widely used and simpler NH_4-N load ratio for predicting the performance of a (bio)electrochemical nutrient removal and recovery system.

1. Introduction

Nitrogen (N), along with other macronutrients potassium (K) and phosphorus (P), are essential for plant growth. For this reason, they are extensively used as fertilisers in agriculture. However, the production of ammonium nitrogen (NH_4-N) for fertiliser purposes requires significant fossil energy inputs, resulting in gaseous emissions [1]. A more efficient method for recycling existing nitrogen is therefore needed. Notably, up to 30% of the nitrogen used as fertiliser ends up in municipal wastewaters [1–3], from where it could be recovered for re-use.

At conventional municipal wastewater treatment plants (WWTPs), a fraction of influent nitrogen is assimilated into the activated sludge used in the treatment process [4,5]. Excess activated sludge is often anaerobically digested, which re-solubilises the biomass-bound nitrogen. After dewatering the digested sludge, nitrogen is mostly present in the liquid fraction called reject water [5]. With nitrogen concentrations typically around 1 $g_{NH4\text{-}N}$ L^{-1}, reject waters are the most nitrogen-rich streams at WWTPs, although their volumes are only < 5% that of the influent wastewater [5–7]. The nitrogen-rich reject waters are commonly recirculated back to the activated sludge process of the WWTP for nitrogen removal, which can contribute up to 25% of the total nitrogen load to the process [6,8] and, consequently, to the energy demand and cost of treatment. Nitrogen removal and recovery (NRR) from reject waters could benefit the energy balance of wastewater treatment and facilitate nitrogen recycling back to agriculture.

In recent years, (bio)electrochemical systems ((B)ESs) have been extensively studied for NRR from reject waters [5,9–12]. In BESs, electroactive bacteria catalyse anodic oxidation reactions, whereas in electrochemical systems (ESs), purely electrochemical reactions take place. In both cases, the generated electric current functions as the driving force for the migration of charged ions over ion-exchange membranes (IEMs), which can be utilised for concentrating NH_4-N. This often takes place in a two-chamber setup with an anode and a cathode chamber separated by a cation-exchange membrane (CEM), which allows the

Abbreviations: AD, Anaerobic digestion; AEM, Anion-exchange membrane; BEC, Bioelectroconcentration cell; BES, Bioelectrochemical system; CEM, Cation-exchange membrane; EC, Electric conductivity; ES, Electrochemical system; IEM, Ion-exchange membrane; NRR, Nitrogen removal and recovery; $R_{a,c}$, Air-to-liquid ratio in the stripping column; sCOD, Soluble chemical oxygen demand; WWTP, Wastewater treatment plant.

* Corresponding author at: Faculty of Engineering and Natural Sciences, Tampere University, Korkeakoulunkatu 8, 33720 Tampere, Finland.
E-mail address: veera.koskue@tuni.fi (V. Koskue).

https://doi.org/10.1016/j.jece.2021.106286
Received 23 June 2021; Received in revised form 24 August 2021; Accepted 25 August 2021
Available online 28 August 2021
2213-3437/© 2021 The Author(s). Published by Elsevier Ltd. This is an open access article under the CC BY-NC-ND license (http://creativecommons.org/licenses/by-nc-nd/4.0/).

concentration of the positively charged NH_4^+ from the anode to the cathode [13]. Alternatively, an anion-exchange membrane (AEM) can be added to create a separate concentrate chamber between the anode and the cathode [9,14–16]. In this three-chamber setup, electric current is used to produce a concentrated liquid nutrient product. This method is called (bio)electroconcentration [9,15,16]. Reject water has shown specific potential for NRR in a three-chamber bioelectroconcentration cell (BEC) with an NH_4-N recovery efficiency of 53 ± 4% from real reject water [9] compared with 50 ± 2% from synthetic urine [14] and 12 ± 1% from real wastewater [16] in a similar setup. Utilising biocatalysts in BESs typically decreases the energy consumption compared with ESs. However, the current generation depends on the amount and biodegradability of the organic content of the feed [17], which is the challenge when working with reject water [5]. This limits the extent of NH_4-N concentration through the IEM, which is largely controlled by the current density [10,18,19].

Furthermore, nitrogen concentration in a (B)ES is often followed by ammonia (NH_3) stripping, a well-established NRR method. In stripping, the pH of the NH_4-N-containing solution is increased to turn soluble NH_4^+ into volatile NH_3 (pKa 9.25). NH_3 can be stripped from the solution into the gas phase by sparging highly dispersed gas through it [4,20]. Traditionally, increasing the pH requires chemical addition. However, in (B)ESs, cathodic reduction reactions release hydroxide (OH^-), thereby increasing the catholyte pH. Thus, the NH_4-N concentrated from the anode chamber to the cathode speciates into NH_3 that can be removed by stripping, followed by re-solubilisation into an acidic solution [5,10]. Even if the stripping step is efficient in removing NH_3 from the liquid phase (up to 100%), the concentration of NH_4-N into the catholyte often limits the total nitrogen recovery [10], unless the reject water is fed directly to the cathode [5]. Notably, the main focus of NRR studies is typically the created nutrient product [5,10,12,21], while the effluent quality of the NRR process and the potential additional treatment it might require are seldom discussed. Alternatively, studies resulting in an effluent quality that eliminates the reject water recirculation within a WWTP have been carried out using simplified synthetic reject water formulations [22].

The objective of this research was to study a novel electrochemical NRR setup in which NH_3 stripping and NH_4^+ electroconcentration were combined and worked cooperatively in recovering nitrogen. Two different NH_4-N product streams were created: the stripped and absorbed nitrogen recovered as an ammonium sulphate solution and a nitrogen-rich liquid concentrate. The aim was to maximise the total nitrogen removal and recovery efficiencies from real reject water. In addition, special attention was allocated to the NRR effluent quality to dispense with the need for additional nitrogen removal treatment.

2. Materials and methods

Short-term preliminary experiments were carried out in smaller-scale laboratory reactors with synthetic reject water. These were performed to determine the optimal NH_4-N load ratio, that is, the ratio between NH_4-N loading rate and applied current (see Section 2.4), to obtain maximal NH_4-N removal efficiency and minimise NH_4-N concentration in the effluent. For more details, see Appendix A in the Supplementary material. The results from these preliminary experiments were used to select the operational parameters for the experiments described in the following sections.

2.1. Experimental setup and media composition

The experiments were carried out in duplicate lab-scale reactors combining electroconcentration and stripping, with electrochemical advanced oxidation taking place at the anode (Fig. 1). The three-chamber electroconcentration unit was made from polycarbonate plates with all three chambers (anode, concentrate and cathode) measuring 5 cm × 20 cm × 1.2 cm. A 40.5 cm^2 DIACHEM® boron-doped

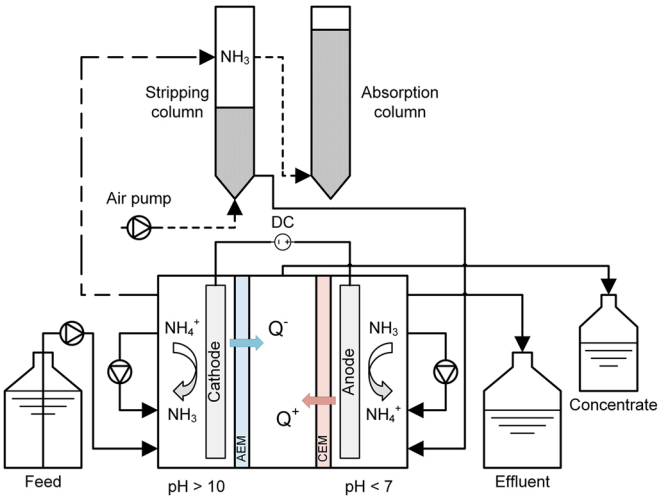

Fig. 1. Schematic presentation of the laboratory-scale setup combining electroconcentration and stripping. Solid lines represent liquid flows and dashed lines gas flows. AEM: anion-exchange membrane; Q^-: anions; Q^+: cations; CEM: cation-exchange membrane.

diamond electrode (Condias GmbH, Germany) connected to a niobium or stainless steel rod was used as anode and a 100 cm^2 piece of AISI 316L stainless steel sintered fibre felt (Xinxiang Lier Filter Technology Co. Ltd, China) with titanium wire as cathode. A cation-exchange membrane (CEM; CMI-7000, Membranes International, USA) was placed between the anode and the middle chambers and an anion-exchange membrane (AEM; AMI-7100, Membranes International, USA) between the cathode and the middle chambers. The effective surface areas of the membranes were 100 cm^2. They were soaked overnight in 5% (w/w) NaCl solution prior to use. Rubber gaskets (1.5 mm thick) were used between the chamber plates and membranes to make the system liquid and airtight, which slightly increased the chamber volumes. The middle chamber was filled with glass beads (6 mm diameter; washed in 1 M HCl overnight prior to use) to prevent membrane distortion. The final hydraulic volumes of the chambers were 133 ± 2 mL for the anode, 119 ± 2 mL for the cathode and 79 ± 1 mL for the middle chamber.

In both duplicate setups, the stripping column was a glass column (3 cm diameter, 53 cm height) filled with K1-type media carriers (Evolution Aqua, UK) up to 25 cm. The liquid volume in the column was 50 mL. An additional glass column (2 cm diameter, 39 cm height) was filled with aquarium filter wool (Aqua One, Australia) and a known volume of 5 M H_2SO_4 and used as an absorption column. The K1 carriers and the aquarium filter wool were used to slow down the gas flow velocity in the columns to maximise contact time with the liquid.

Both synthetic and real reject water were utilised as feed. First, a synthetic formula was used, mimicking real reject water characterised previously [9] and containing (in mg L^{-1}) Na_2HPO_4 (104), $MgCl_2{\cdot}6H_2O$ (231), $CaCO_3$ (152), $KHCO_3$ (274), NH_4HCO_3 (3751), CH_3COONa (111) and C_2H_5COOH (52). Thereafter, real reject water was collected from Luggage Point municipal WWTP (Brisbane, Australia), which contained on average (in mg L^{-1}) NH_4-N (983 ± 50), PO_4-P (7.3 ± 1.9), K (221 ± 11), Na (341 ± 19), Ca (36 ± 4), Mg (18 ± 7), Cl (656 ± 25), inorganic carbon (752 ± 59) and organic matter, expressed as soluble chemical oxygen demand (sCOD; 853 ± 416), out of which 297 ± 100 mg L^{-1} were acetate and 44 ± 11 mg L^{-1} were propionate. The total suspended solids (TSS) of the real reject water were 191 ± 52 mg L^{-1}. To avoid blockages in the operational setup, the solids in the reject water were allowed to settle at the bottom of the storage canisters. Then, the feed was decanted from the canisters into a feed bottle without any further pre-treatment. The reject water was stored at +4 °C for a maximum of one week. A fresh batch of feed was collected from the cold room daily and kept in room temperature for a maximum

of 24 h.

2.2. Reactor operation

Synthetic or real reject water was continuously fed to the cathode chamber of the electroconcentration unit (Fig. 1). At the cathode, protons were reduced to hydrogen gas, which increased the catholyte pH and turned the influent NH_4^+ to volatile NH_3, while anions were able to migrate through the AEM into the concentrate chamber. The catholyte–hydrogen gas mixture continued into the stripping column for gas–liquid separation. The liquid fraction was collected from the bottom of the stripping column and fed to the anode of the electroconcentration unit. Here, protons were generated as a result of oxidation reactions. The resulting low pH turned the remaining NH_3 back to NH_4^+, which was able to migrate to the concentrate chamber over the CEM together with other cations. The effluent from the anode was collected into an effluent bottle. Simultaneously, water was also flowing into the concentrate chamber due to osmotic and electro-osmotic forces. The formed liquid concentrate was collected as overflow into a concentrate bottle. The catholyte and anolyte were circulated in the respective chambers at 35 mL min^{-1} (except for the final experiment in which the rate was increased to 105 mL min^{-1}) to reduce mass transfer limitations. For the final experiment with real reject water (R4; see Table 1), mixing was also applied to the middle chamber at a rate of 105 mL min^{-1} to avoid the formation of high local concentration gradients near the membrane surfaces.

Air was bubbled into the stripping column from the bottom through a glass frit at 12 ± 1 mL min^{-1} to strip volatile NH_3 from the liquid (Fig. 1). The gas mixture was collected at the top of the stripping column and bubbled through H_2SO_4 to re-solubilise and, thus, capture the stripped NH_3. Watson-Marlow Sci-Q 323 peristaltic pumps (Watson-Marlow Fluid Technology Group, United Kingdom) were used for both liquid and gas pumping. A laboratory DC power supply (IPS 2303, ISO-TECH) was used to apply a constant current of 0.35 or 0.7 A, corresponding to a current density of 35 or 70 A m^{-2} relative to the effective membrane surface area (or ca. 86 or 173 A m^{-2} to anode surface area). The power supply also measured cell voltage. Cell voltage was recorded when sampling, while individual electrode potentials were not recorded. All experiments were carried out in ambient temperature (22 ± 2.5 °C) and pressure.

Five different experiments were carried out: one with synthetic reject water (S1) and four with real reject water (R1–R4; Table 1). For run S1, the NH_4-N load ratio was matched with the load ratio leading to the highest total NH_4-N removal and the lowest effluent concentration in the smaller-scale preliminary experiments (Fig. A.1 in Supplementary material). Runs R1–R3 with real reject water were designed to reproduce the NRR efficiency obtained with synthetic reject water by matching the different operational parameters to those of S1: the feed rate and, thus, the hydraulic retention time (HRT); the NH_4-N loading rate and, thus, the NH_4-N load ratio; and the cation loading rate and, thus, the cation load ratio (Table 1). The aim of the final real reject water run, R4, was to determine the highest obtainable NH_4-N removal and recovery by significantly increasing the NH_4-N (and cation) load ratio. This was done by simultaneously decreasing the feed rate and increasing the current density. In addition, the mixing rate for the anode and cathode chambers was tripled to 105 mL min^{-1} to eliminate mass transfer limitations. The ratio between the air and liquid flows in the stripping column ($R_{a,c}$; see Section 2.4) increased with decreasing feed rate (Table 1).

2.3. Sampling and chemical analyses

Samples for the elemental analyses (NH_4-N, PO_4-P), soluble ions (K^+, Na^+, Mg^{2+}, Ca^{2+}, Cl^-), sCOD, volatile fatty acids (VFAs) and total inorganic carbon (TIC) were taken from the feed, cathode effluent, anode effluent and concentrate three times with 24 h sampling intervals once the reactors had been operated for at least four HRTs and were considered to be in steady state (i.e., the electric conductivity (EC) of the concentrate and effluent were stable). In addition, samples were taken from the absorption columns to analyse the absorbed NH_4-N. EC and pH were measured immediately after sampling using LAQUAtwin probes EC-22 and pH-22 (Horiba Scientific, Japan), respectively. Samples were filtered through Millex® syringe filters (pore size 0.22 μm; Merck Millipore, Germany) and stored at −20 °C for further analyses.

The NH_4-N and PO_4-P were analysed with a Flow Injection Analyser (FIA) (Lachat Quikchem 8500 Series 2; Hach, USA); the NH_4-N in the acid trap with the Total Kjeldahl Nitrogen (TKN) method using the FIA; the cations (K^+, Na^+, Mg^{2+} and Ca^{2+}) with an Inductively Coupled Plasma-Optical Emission Spectrometer (ICP-OES) (Optima 7300DV; PerkinElmer, USA) after nitric acid digestion; the Cl^- with an Ion Chromatography System (Dionex ICS-2000, Thermo Fisher Scientific, USA); the VFAs with a Gas Chromatography System (7890A, Agilent Technologies, USA); the TIC with a Total Organic Carbon Analyser TOC-L CSH with TNM-L TN unit (Shimadzu, Japan); and the sCOD with Spectroquant® COD test kits (Merck Millipore, Germany). TSS for the real reject water was determined according to standard SFS-EN 872:2005 [23].

2.4. Calculations

Removal and recovery efficiencies (%) for different ions were calculated by comparing the concentrations in the effluent, concentrate and absorption column (only for NH_4-N) to the influent concentrations. Effluent and concentrate volumes were measured to obtain accurate mass balances. The reported values are mean values of the two reactors in three sampling points ($n = 6$) with standard deviations (±) unless stated otherwise. As the stripping and absorption contributed little to NH_4-N removal (as discussed in Section 3.4), the removal rates of all compounds including NH_4-N were normalised to the total theoretical electroconcentration reactor volume (360 mL; g m^{-3} d^{-1}), i.e., excluding stripping column volume, or effective membrane surface area (100 cm^2; g m^{-2} d^{-1}). To determine the electrical energy required for NH_4-N removal, the power consumption was calculated from the current and voltage data normalised to the duration of each sampling period and the mass of NH_4-N removed over it.

The transport efficiency tE_n (%) or the contribution of an ion to the total charge transport over a membrane was calculated as reported previously [24]:

Table 1
Operational parameters of the five experimental runs. Hydraulic retention times (HRTs) are normalised to the combined hydraulic volumes of the anode and cathode chambers and current densities to the effective membrane surface area. NH_4-N and cation load ratios refer to the ratio between applied current and NH_4-N or cation loading rate, respectively. $R_{a,c}$ refers to the ratio between the air and liquid flows in the stripping column.

Experiment	Origin of reject water	Feed rate [L d^{-1}]	HRT [h]	NH_4-N loading rate [mmol L^{-1} d^{-1}]	Cation loading rate [mmol L^{-1} d^{-1}]	J [A m^{-2}]	NH_4-N load ratio [-]	Cation load ratio [-]	$R_{a,c}$ [-]
S1	Synthetic	2.8	2.2	513	598	35	2.4	2.1	6
R1	Real	2.8	2.2	811	1075	35	1.6	1.1	6
R2	Real	1.8	3.3	527	693	35	2.4	1.8	10
R3	Real	1.5	4.1	410	535	35	3.1	2.3	12
R4	Real	0.6	10.3	152	198	70	16.0	11.7	30

$$tE_n = \frac{\frac{J_n}{M_n} * z_n * F}{j_{applied}} * 100\% \quad (1)$$

where n is the studied compound, J_n is the removal rate of the compound (g m^{-2} s^{-1}, normalised to effective membrane surface area), M_n is the molar mass of the compound (g mol^{-1}), z_n is the charge of the compound, F is the Faraday constant (96,485 C mol^{-1}) and $j_{applied}$ is the current density (A m^{-2}).

The NH_4-N load ratio L_N (-) was also calculated as reported previously [19]:

$$L_N = \frac{j_{applied}}{c_{NH4-N,\ feed} * Q_{feed} * \frac{F}{A_m}} \quad (2)$$

where $c_{NH4\text{-}N,\ feed}$ is the NH_4-N concentration in the feed (mol m^{-3}), Q_{feed} is the feed rate (m^3 s^{-1}) and A_m is the effective membrane surface area (m^2).

The concept of a cation load ratio L_C (-) was introduced and calculated as modified from Eq. (2) as follows:

$$L_C = \frac{j_{applied}}{\sum_{i=1}^{n}(c_i * z_i) * Q_{feed} * \frac{F}{A_m}} \quad (3)$$

where c_i is the concentration of a cation in the feed (mol m^{-3}) and z_i is the charge of the cation.

For ammonia stripping, the ratio between the air and liquid flows in the stripping column can be expressed as reported previously [25]:

$$R_{a,c} = \frac{Q_{air}}{Q_{catholyte}} \quad (4)$$

where Q_{air} is the air flow (mL min^{-1}) fed into the stripping column and $Q_{catholyte}$ is the flow of liquid (mL min^{-1}) from the cathode to the stripping column.

Statistical analyses were carried out using Microsoft Excel Data Analysis and a 5% significance threshold. Two-sample *t*-tests were used to check the similarity between the data sets of the duplicate reactors. Regression analysis was used to find linear trends and spot outliers.

3. Results and discussion

3.1. NH_4-N removal and recovery

3.1.1. NH_4-N was efficiently removed from synthetic and real reject water

Preliminary runs were used for the optimisation of the NH_4-N load ratio with synthetic reject water, with the highest NH_4-N removal of 93 ± 1.4% at NH_4-N load ratio of 2.5 (see Fig. A.1 in Supplementary material). In run S1, using slightly larger reactors and modified stripping and absorption columns, the selected NH_4-N load ratio 2.4 led to an even higher NH_4-N removal of 97 ± 2.3% with synthetic reject water, corresponding to an NH_4-N removal rate of 5.9 ± 0.3 kg_N m^{-3} d^{-1} (Fig. 2). With real reject water and a matching feed rate and HRT to S1, resulting in a lower NH_4-N load ratio of 1.6 (R1), the NH_4-N removal efficiency was significantly lower at 73 ± 6.7%, even if the removal rate increased to 6.8 ± 0.8 kg_N m^{-3} d^{-1}. When the NH_4-N load ratio was matched to that of S1 with real reject water (R2), the removal efficiency increased to 81 ± 22% and further to 90 ± 6.9% by matching the cation load ratio (2.3 in R3 vs. 2.1 in S1). In the final run with real reject water (R4), where the NH_4-N load ratio was more drastically increased (see Table 1), the obtained NH_4-N removal efficiency was the highest at 94 ± 0.4% and very close to the 97 ± 2.3% obtained with synthetic reject water. Overall, the NH_4-N removal efficiency from real reject water increased linearly as a function of both NH_4-N and cation load ratios ($R^2 > 0.98$ for both) when run R4 that had a clearly larger load ratio than the 'limiting' load ratio is excluded (see Fig. 3 and Section 3.2 for details). Conversely to the NH_4-N removal efficiency, the removal rate decreased from 6.8 ± 0.8 to 1.7 ± 0.02 kg_N m^{-3} d^{-1} (Fig. 2) with decreasing NH_4-N load ratio with real reject water.

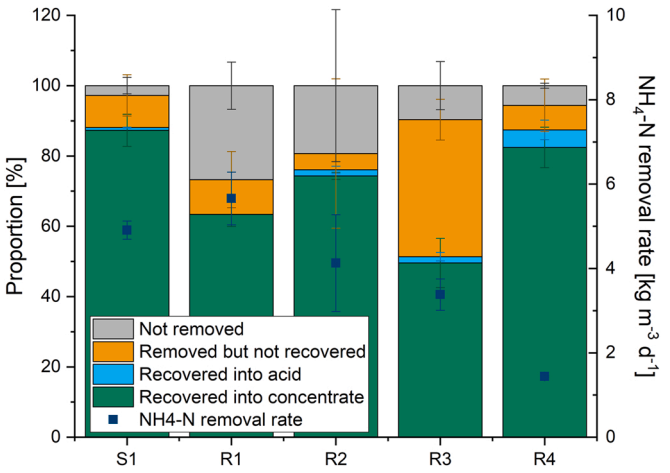

Fig. 2. NH_4-N mass balances and removal rate in the different experiments with synthetic (S1) and real (R1–R4) reject water (for experimental parameters, see Table 2). For R1, recovery into acid was not determined. For R4, results from only one of the duplicate reactors are presented due to operational issues with the other reactor, resulting in dissimilar behaviours of the two reactors ($P < 0.05$ based on the two-sample T-test).

The removed NH_4-N was also efficiently recovered. Almost all of the NH_4-N recovery took place via ion migration into the concentrate chamber in the electroconcentration step, while stripping and absorption played a very minor role in the recovery (< 5%, Fig. 2), as discussed in the following sections.

3.1.2. Removed NH_4-N was effectively recovered into a liquid concentrate

The NH_4-N recovery efficiency from synthetic reject water into the liquid concentrate was 87 ± 4.6% (S1), whereas a similar NH_4-N load ratio resulted in a lower recovery efficiency of 74 ± 1.0% with real reject water (R2). The recovery efficiency into concentrate peaked at 82 ± 5.7% with real reject water (run R4) (Fig. 2). At the same time, the NH_4-N concentrations in the concentrate peaked at 15.3 ± 0.5 and 19.0 ± 0.7 g L^{-1} with synthetic and real reject water, respectively (Table 2).

With a matching cation load ratio (run R3), the NH_4-N recovery efficiency was considerably lower compared with the other runs at 51 ± 8.2%, meaning that up to 39% of the influent NH_4-N was lost in the system. The two-sample T-test indicated that the duplicate reactors behaved similarly (P values of 0.49 for NH_4-N removal and 0.34 for NH_4-N recovery), but a regression analysis comparing the averaged concentrate production rate (results not shown) to the NH_4-N load ratio showed that R3 was a clear outlier from an otherwise linear trend in the real reject water experiments ($R^2 = 0.08$ for R1–R4 compared with $R^2 = 0.96$ for R1, R2 and R4). As a similar loss was also observed for potassium and sodium in R3 (see Fig. B.1C in Appendix B, Supplementary material), the large NH_4-N loss was attributed to a leakage from the middle chambers of the reactors and an anomaly in the recovery results.

The obtained NH_4-N recoveries into the concentrate are the highest reported to date for a three-chamber (bio)electroconcentration cell operated with different nutrient-rich streams [9,14–16]. Even though the NH_4-N removal and recovery efficiencies from real reject water (up to 94 ± 0.7% and 82 ± 5.7%, respectively) were slightly lower than those from the simpler synthetic composition (97 ± 2.3% and 87 ± 4.6%, respectively), the obtained removal and recovery efficiencies were high and notably improved compared with our earlier work in a biological NRR unit [9], where the highest obtained recovery efficiencies were 76 ± 4.6% from synthetic and 53 ± 4.0% from real reject water. The major reason for this was the higher applied current

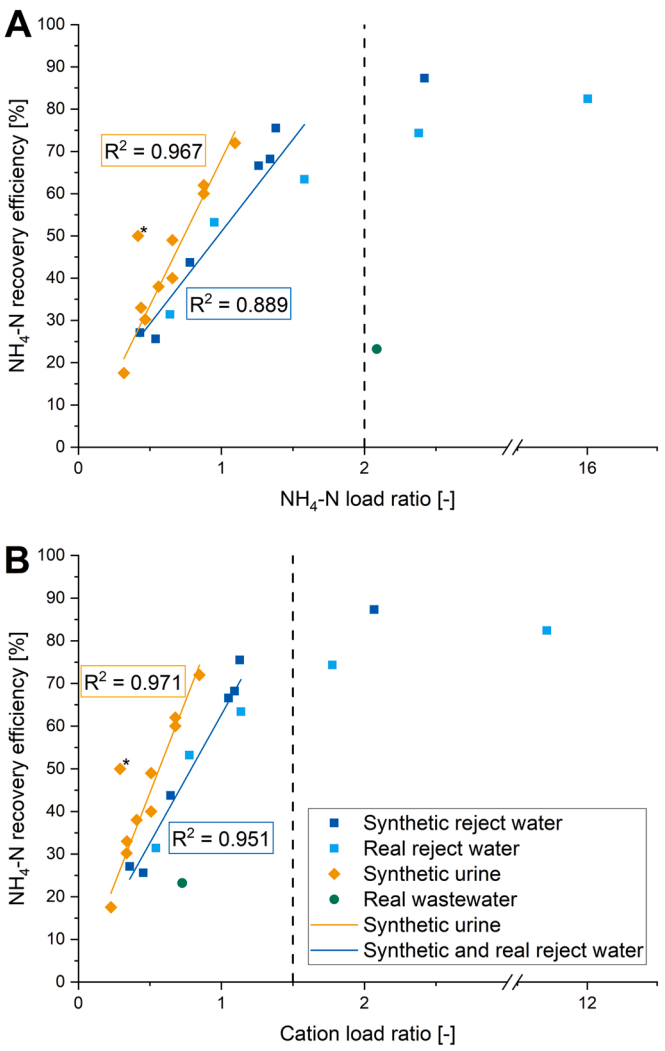

Fig. 3. NH_4-N recovery efficiencies as a function of (a) NH_4-N load ratio and (b) cation load ratio. Data were compiled from different studies using a similarly structured three-chamber (B) EC fed with different nutrient-rich feed streams [9,14–16,29]. Linear trendlines were fitted to the linearly increasing parts of the synthetic urine (yellow) and synthetic and real reject water (blue) data sets. For synthetic and real reject water, the roughly estimated limiting load ratios were marked with dashed lines. For synthetic urine, the data point marked with an asterisk (*) [14] was excluded from both fittings as an outlier. (For interpretation of the references to colour in this figure legend, the reader is referred to the web version of this article.)

Table 2
NH_4-N concentrations in the feed, effluent and concentrate in the different experiments, as well as up-concentration factors (i.e., ratio of the concentration in the concentrate compared to the feed).

Experiment	$c_{NH4\text{-}N,feed}$ [mg L^{-1}]	$c_{NH4\text{-}N,effluent}$ [mg L^{-1}]	$c_{NH4\text{-}N,concentrate}$ [g L^{-1}]	Up-concentration factor [-]
S1	647 ± 2	18 ± 16	15.3 ± 0.5	24 ± 0.9
R1	1006 ± 18	274 ± 67	19.0 ± 0.7	19 ± 0.8
R2	1030 ± 8	207 ± 231	15.8 ± 0.2	15 ± 0.3
R3	977 ± 39	99 ± 71	12.7 ± 0.7	12 ± 2.4
R4	913 ± 14	57 ± 7	6.6 ± 0.4	7.3 ± 0.5

density (35 or 70 A m^{-2} compared with ≤ 4.8 A m^{-2}, relative to the effective membrane surface area), which means a higher driving force for electromigration. In the biological system, the amount of biodegradable organics often limits the current generation [5,17], which can be overcome in a purely electrochemical system that was also used in the current study.

In addition, NH_4-N recovery efficiencies of 50 ± 1.8% from synthetic hydrolysed urine [14] and 12 ± 1.4% from real domestic wastewater [16] in a similarly structured three-chamber BEC are considerably lower than those reported here. In an abiotic three-chamber electroconcentration cell operated with synthetic hydrolysed urine, the maximum NH_4-N recovery into the liquid concentrate was 72 ± 1% with high current densities up to 100 A m^{-2} [15] compared with the 35 and 70 A m^{-2} applied here. The higher NH_4-N concentration of synthetic urine resulted in the NH_4-N load ratio remaining below 1.1 in all experiments [15], which likely explains the higher recovery efficiencies obtained in this study using higher NH_4-N load ratios. In general, NH_4-N recovery efficiencies tend to be higher with synthetic urine than with synthetic or real reject water at matching NH_4-N load ratios in the studied three-chamber NRR unit (Fig. 3A). However, in this study, the NH_4-N load ratios were high enough to increase the recovery efficiency beyond what has been obtained with synthetic urine in the past.

The obtained NH_4-N removal and recovery efficiencies are also very competitive compared with other recent membrane-based NRR research using digested sewage sludge reject water. Recently, stacked electrochemical membrane systems utilising bipolar membranes (BPMs) and CEMs were found to remove up to 80% of NH_4-N from synthetic reject water in continuous operation [12] and up to 88% from real reject water in batch operation [21]. The results obtained here also outweigh many nitrogen removal and recovery studies using synthetic or real source-separated urine, with reported removal and recovery efficiencies typically in the range of 51–82% [24,26–28]. In some cases, even complete NH_4-N removal has been reported from reject water [22] or urine [19], but these results have been obtained using simplified synthetic formulas. Here, high NH_4-N removal and recovery efficiencies were obtained from real reject water using only settling as a simple pre-treatment.

3.1.3. Stripping and absorption were a minor contribution to NH_4-N recovery

As previously mentioned, the stripping and absorption step contributed very little (≤ 5.0 ± 2.8%) to the total NH_4-N removal and recovery in the NRR unit (Fig. 2). Earlier studies have shown that stripped NH_3 gas efficiently absorbs into an acidic solution [5,30]. Therefore, it was concluded that the stripping step in the current study was inefficient. As the catholyte pH was ≥ 10 in all experiments (Fig. B.3 in Supplementary material), which was adequate for efficient stripping [25], it was concluded that the selected $R_{a,c}$ values of 6–30 (Table 1) were too low to facilitate NH_3 stripping.

The $R_{a,c}$ values in this study were set at a low level as the aim was never to recover all of the NH_4-N via stripping and absorption. Moreover, values in a similar range (25–45) have previously been used in a study combining electrochemical NH_4-N concentration and stripping using real reject water [10]. Conversely to this study, similar $R_{a,c}$ values were found previously to lead to high stripping efficiencies of up to 100% from real reject water (even though the concentration step limited the total NH_4-N recovery to ≤ 63%) [10]. It should be noted, however, that the low instantaneous $R_{a,c}$ used by Desloover et al. was compensated with increased contact time by recirculating the catholyte over the stripping column and cathode chamber [10]. Indeed, even though the reported $R_{a,c}$ was 25–45 against the catholyte recirculation rate, the real $R_{a,c}$ values were as high as 7200–12,960 when comparing the total air volume coming to contact with the total catholyte volume [10]. Similarly, in another earlier work combining electrochemical NH_4-N concentration and stripping, a 20 h period of stripping in batch mode was required to obtain 79% NH_4-N recovery from real reject water, resulting in an $R_{a,c}$ value of 3600 [5]. To achieve efficient NH_3 stripping, the $R_{a,c}$ values used here would have to be increased notably by either raising the air flow rate or by increasing the contact time with the catholyte via methods such as catholyte recirculation. In fact, it has been suggested

that the optimal air to liquid ratio $R_{a,c}$ for effective NH_3 stripping could be 1500–2000 [25].

However, as the obtained total NH_4-N removal and recovery were already high, no further effort was made to optimise the performance of the stripping column within the scope of this study. As almost all of the NH_4-N removal and recovery took place via electroconcentration, the stripping and absorption columns could be completely removed from the system, making it fully chemical-free. Alternatively, the stripping column could potentially be utilised for separating the hydrogen gas that is continuously produced at the cathode as a result of reduction reactions from the liquid phase. Hydrogen has a much lower solubility in water (1.62 mg L^{-1}) compared with NH_3 (540,000 mg L^{-1}) [31] and it is up to five orders of magnitude more volatile [32], so it would be easier to strip hydrogen from the liquid phase. The separated hydrogen gas could be recycled to the AD process to upgrade the produced biogas into biomethane [33], which could further favour the energy balance of the full WWTP and AD system.

3.2. Competing cations and the concept of cation load ratio

Overall, the NH_4-N removal and recovery results followed previously reported trends: (1) with increasing NH_4-N load ratio, the removal and recovery efficiencies increased while the removal rate decreased [9,27] and (2) an identical NH_4-N load ratio compared to the run with synthetic reject water did not lead to NH_4-N removal and recovery that were as efficient as those with real reject water (S1 vs. R2; Fig. 2) [9,19]. The increase in removal and recovery efficiencies can be explained by changing the load ratio mainly by altering the feed rate. A slower feed rate leads to a higher load ratio and HRT, enabling longer contact times and, thus, more efficient removal and recovery. At the same time, a longer HRT indicates that new NH_4-N becomes available at a slower rate, which is also reflected in the slower removal rate. The latter observation, on the other hand, can be explained by the fact that ion-exchange membranes are not NH_4^+-specific. Therefore, the varying ratios of other cations to NH_4-N in different wastewater streams greatly affect the NH_4-N removal and recovery efficiency in a membrane-based NRR system. This underscores that the NH_4-N load ratio alone is not a robust method to predict the NH_4-N removal and recovery efficiencies in an NRR system used for varying feed streams of complex and changing composition.

Given the foregoing, the cation load ratio, that is, the ratio between applied current and the combined loading rate of NH_4^+, K^+, Na^+, Mg^{2+} and Ca^{2+} (Eq. (3)), was matched with real reject water (R3) to that of S1. As the main NH_4-N removal mechanism was electromigration over the CEM and other cations compete with NH_4^+ for the charge transport, it was hypothesised that the other cations play an important role in the NH_4-N removal and recovery efficiency. Indeed, with a matching cation load ratio, the obtained NH_4-N removal efficiency increased to 90 ± 6.9% (from 81 ± 22% with a matching NH_4-N load ratio) with real reject water, which was much closer to the 97 ± 2.3% obtained with synthetic reject water. The NH_4-N recovery results between these runs were not comparable, as discussed previously. Therefore, the results from R3 were excluded from Fig. 3.

When inspecting the NH_4-N recovery efficiencies obtained in three-chamber (B)ECs as functions of both NH_4-N load ratio and cation load ratio (Fig. 3), some interesting observations can be made. First, both the synthetic urine and synthetic and real reject water data seem to follow a linearly increasing trend at the beginning, after which the reject water results start to level off at NH_4-N load ratio of ca. 2 or cation load ratio of ca. 1.5 (marked with dashed lines in Fig. 3). This trend has been reported before and referred to as 'limiting load ratio', after which increasing the load ratio further offers little additional benefit with regards to the recovery efficiency [19]. When applying a linear fitting into the linearly increasing part of the combined synthetic and real reject water dataset, using cation load ratio gives a better fit ($R^2 = 0.951$ vs. $R^2 = 0.889$ with NH_4-N load ratio). At the same time, the real wastewater data point is grouped much more closely to the other data points when looking at the cation load ratio, even though it is a clear outlier when only the NH_4-N load ratio is examined. The linear fittings for the synthetic urine data points are of equal quality with both NH_4-N and cation load ratios. Thus, Fig. 3 suggests that the cation load ratio is a better parameter than the more widely applied NH_4-N load ratio for estimating removal and recovery efficiencies in (bio)electrochemical NRR systems. However, more comprehensive analyses with larger data sets are required to fully understand its potential.

Despite the presence of competing cations, NH_4^+ was the main charge carrier over the CEM (see Fig. B.2 in Supplementary material), contributing up to 36% of the charge transport over the CEM with synthetic and 40% with real reject water at the lowest NH_4-N load ratio. The contribution of NH_4^+ and other measured cations declined with increasing NH_4-N load ratio due to the decreased pH at the anode (see Fig. B.3 in Supplementary material), which increased the concentration of H^+ in the anolyte and, thus, its share of the charge transport, a trend observed previously [12,27,34].

Potassium, another key macronutrient, was efficiently recovered into the liquid concentrate simultaneously to NH_4-N at a maximum efficiency of 89 ± 3.4% from synthetic and 88 ± 6.8% from real reject water (see Fig. B.1 in Supplementary material). Similarly, a competing monovalent cation sodium was recovered with recovery efficiencies up to 95 ± 3.2% from synthetic and 91 ± 7.6% from real reject water. The divalent cations magnesium and calcium, on the other hand, were mostly lost in the system: effectively removed but not recovered into the concentrate. This was likely due to the precipitation of magnesium and calcium compounds in the alkaline conditions at the cathode, a known phenomenon [35,36]. The formed precipitates were not elementally analysed but the formation of calcite ($CaCO_3$), hydroxyapatite ($Ca_5(PO_4)_3OH$) and struvite ($NH_4MgPO_4{\cdot}6H_2O$) was confirmed through Aqion and Visual MINTEQ software modelling (results not shown).

3.3. Potential for eliminating the need for additional nitrogen removal treatment

The efficient NH_4-N removal from synthetic reject water resulted in low NH_4-N concentrations of 18 ± 16 mg L^{-1} in experiment S1 (Table 2). With real reject water, the effluent NH_4-N concentration decreased with increasing NH_4-N load ratio from 274 ± 67 to 57 ± 7 mg L^{-1}.

With the lowest NH_4-N effluent concentrations, the treated reject water would potentially require no further treatment for additional NH_4-N removal, that is, it could be discharged as such or via tertiary treatment. Even if the effluent concentrations may be slightly above case-specific discharge limits, it should be kept in mind that the effluent from the NRR system would be discharged with the effluent of the WWTP. The WWTP effluent volume is ca. 100 times the volume of the reject water [6]. Therefore, the NRR effluent would be significantly diluted at discharge, bringing NH_4-N concentrations $\leq$ 3 mg L^{-1} in all studied cases. For example, at the Luggage Point WWTP (Brisbane, Australia), where the real reject water used in this work was obtained, the NH_4-N discharge limit is 4 mg L^{-1} (as a long-term median value) [37]. This means that the effluent from the NRR unit could bypass recirculation to the activated sludge process and be directed to the tertiary treatment of the WWTP, or possibly even directly discharged depending on other effluent discharge limits, which are mainly phosphorus and biological oxygen demand (BOD).

Here, the real reject water from the WWTP contained very little phosphorus to begin with (7.3 ± 1.9 mg L^{-1} on average), as most of the phosphorus remains in the solid fraction of the digested sewage sludge after precipitation with ferric chloride [38]. In all experiments, the NRR effluent concentrations for phosphorus were $<$ 2.3 ± 0.4 mg L^{-1}.

BOD was not determined but sCOD was measured from the influent and effluent of the NRR unit in runs R2 and R4, giving an indication of the fate of the organic matter. The sCOD removal efficiency increased

from 74 ± 9.8% in R2 to 81 ± 1.8% in R4, corresponding to effluent concentrations of 127 ± 60 and 275 ± 12 mg L^{-1}, respectively. In addition to sCOD, its VFA fractions, namely, acetate and propionate, were measured in all experiments, except for R1, and full mass balances were determined (see Fig. B.1 in Supplementary material). With synthetic reject water (S1; Fig. B.1A), low effluent concentrations for both acetate (7.3 ± 2.0 mg L^{-1}) and propionate (3.9 ± 1.7 mg L^{-1}) were obtained. With real reject water (R2–R4; Fig. B.1B–D), the effluent concentrations remained below 119 ± 14 mg L^{-1} for acetate and 21 ± 1.7 mg L^{-1} for propionate in all experiments. Again, these concentrations would be further diluted at discharge, or tertiary treatment could be used for the removal of the remaining organics.

Alternatively, the NRR effluent could be recycled back to the activated sludge process. With the high NH_4-N removal efficiencies obtained in the NRR unit, the additional NH_4-N load would be minimal, while the remaining COD in the NRR effluent could likely be utilised as carbon source for the denitrification part of the activated sludge process. In denitrification, carbon is required for NH_4-N removal and is often limiting in the influent wastewater, which is why an external carbon addition is required [39]. The recirculation of the NRR effluent to the denitrification process with the remaining organics and little additional NH_4-N load could help facilitate the COD:NH_4-N balance and mitigate the need for the external carbon addition, thereby lowering the operational costs. However, it should be kept in mind that not all of the COD originating from reject waters is easily biodegradable [5].

3.4. Identified additional benefits and challenges

In addition to the points discussed above, the NRR system studied here provided some other benefits worth mentioning. First, as reject water was first fed to the cathode, most of the Cl^- was concentrated into the middle chamber through the AEM (Fig. 1). Thus, the Cl^- levels entering the anode were low (< 172 mg L^{-1} compared with influent concentrations of 656 mg L^{-1} with real reject water). This helps in preserving the NH_4-N in the medium as chloride has been found to readily oxidise at a BDD anode, forming radicals that are capable of destroying the NH_4-N present in the medium when the chloride:NH_4-N ratio is high enough [40]. As discussed previously, the NH_4-N losses were generally low at < 10%, except for run R3 with a leakage (Fig. 2), which indicates that NH_4-N loss caused by chloride radicals was not a considerable issue. Furthermore, chloride oxidation at the BDD has been found to result in the formation of a persistent toxic by-product, namely, perchlorate [40]. Here, perchlorate or other chlorination products were not analysed, but as the initial chloride concentrations at the anode were low, little toxic chloride by-product formation can be expected.

Second, the Mg^{2+} and Ca^{2+} present in the reject water are often favoured as charge transporters over the CEM compared to monovalent cations NH_4^+, K^+ and Na^+ [36]. Consequently, they tend to easily precipitate in the concentrate chamber due to the elevated pH, which causes inorganic scaling on the CEM [36]. Here, magnesium and calcium first went through the alkaline conditions at the cathode, where most of them precipitated. Naturally, the precipitation of magnesium and calcium compounds on the cathode surface or the AEM is also not desirable as it can increase the internal resistance and, in turn, the energy consumption of the system [41]. This is why including a precipitation vessel in the cathode recirculation loop could be considered. In any case, this phenomenon helps protect the CEM from inorganic scaling, thereby maintaining its permeability properties that are crucial for effective NH_4-N recovery.

At the same time, a challenge with using an electroconcentration system is that a high removal efficiency, such as the one reported here, leads to the depletion of ions in the anode and cathode chambers of the system. This decreases the EC to a very low level (here, down to 0.2 and 0.9 mS cm^{-1} at the anode with synthetic and real reject water, respectively). The low EC results in increased ohmic resistance of the electrolyte, leading to high cell voltages and consequent energy consumption. The internal resistance can be further increased by the formation of magnesium and calcium precipitates on electrode and/or membrane surfaces [41]. With synthetic reject water, the electrical energy consumption (excluding pumping) was 91 ± 8.8 kW h kg_N^{-1} removed. Given the higher EC of the real reject water, the energy demand with the corresponding NH_4-N load ratio of 2.4 (R2) was slightly lower at 79 ± 35 kW h kg_N^{-1}. Pumping energy was left out of the energy calculations because for liquid flows in larger scales, it can be expected to be an order of magnitude lower than the electrochemical energy input [11]. Meanwhile, the electricity demand for air pumping can be significant but it was also excluded from the energy calculations, as practically all of the NRR took place via electroconcentration. Therefore, stripping could be excluded from the setup. In general, the energy consumption increased linearly with an increase in the load ratio for the real reject water (Fig.B.4 in Supplementary material). Thus, it is important to establish a compromise between the NH_4-N removal and recovery efficiency and energy consumption.

When normalising the energy consumption to the volume of reject water treated, the energy consumption is almost identical at 57 ± 5.7 kW h m^{-3} and 58 ± 7.5 kW h m^{-3} with synthetic and real reject water, respectively. When normalising the consumed energy to the total wastewater volume flowing through the WWTP (estimating the reject water volume to be 3% of the total wastewater flow), the energy consumption would be around 1.7 kW h m^{-3} at 80% NH_4-N removal (R2) or 2.8 kW h m^{-3} at 90% NH_4-N removal (R3). These values are still high compared with the < 0.6 kW h m^{-3} used by the conventional WWTPs producing adequate quality effluents [42].

The energy consumption of the proposed technology is also high compared to an established reject water treatment method, anaerobic ammonium oxidation or anammox, which typically only uses < 2 kW h kg_N^{-1} [43]. The NH_4-N removal efficiency of anammox, however, can vary quite significantly. For full-scale WWTPs using anammox for treating reject water with ca. 1–1.5 $g_{NH4\text{-}N}$ L^{-1}, the effluent NH_4-N concentrations can vary between 50 and 750 mg L^{-1} [43]. Furthermore, the start-up of an anammox unit is complex and time consuming as it requires a very specific microbial community that is often associated with slow growth rates and sensitivity to environmental changes [44]. The electroconcentration approach presented here involves no biological processes, making the implementation quick and simple and the process more robust to changes in the feed composition. Finally, electroconcentration facilitates the recovery of nitrogen in a reusable form, whereas anammox loses nitrogen into the atmosphere as N_2 gas [44].

Another established nitrogen removal method that is already used in a larger scale, and also facilitates recovery, is traditional air stripping of ammonia. However, as discussed before, air stripping requires the elevation of reject water pH and/or temperature and significant air pumping through the liquid [25], which all add to the chemical and energy requirements of the method. Furthermore, even though the selective recovery of only NH_4-N might be preferable sometimes, ammonia stripping fails to simultaneously recover other key nutrients, such as potassium. Electroconcentration, on the other hand, offers a chemical-free option for recovering all key nutrients into one stream.

Even though the energy demand under the studied conditions was high overall, it should be noted that energy usage was not optimised within the scope of this study. For example, ohmic resistance within the system could be minimised by reducing the electrode distance further [45] or by eliminating magnesium and calcium precipitation through a pre-treatment method [11,35] or an operational strategy [35,36]. Furthermore, the potential benefits from utilising the generated hydrogen gas were excluded from the energy calculation. If the stripping column was only used for hydrogen gas separation, without attempting ammonia stripping, there would also be no need for the absorption column. This would make the NRR system fully reagent-free. Indeed, the NRR unit has the potential to benefit a WWTP in many ways, such as reduced chemical usage and aeration due to reduced NH_4-N load to the

activated sludge process, resulting in decreased sludge generation and pumping requirements, as well as biogas upgrading with the hydrogen gas. Therefore, the effect of the NRR unit on the total energy balance of the WWTP should be evaluated in more detail at an appropriate scale.

4. Conclusions

In this study, the novel NRR unit combining electroconcentration and stripping effectively removed and recovered NH_4-N from both synthetic and real digested sewage sludge reject water. At peak performance, NH_4-N removal was $97 \pm 2.3\%$ from synthetic and $94 \pm 0.7\%$ from real reject water, resulting in effluent NH_4-N concentrations of 18 ± 16 and 57 ± 6.7 mg L^{-1}, respectively. The concentrations were low enough to consider dispensing with any further nitrogen removal treatment for the NRR effluent. The removed NH_4-N was efficiently recovered into a liquid concentrate with up to $87 \pm 4.6\%$ efficiency from synthetic and $82 \pm 5.7\%$ from real reject water, while stripping and absorption contributed little ($\leq$ 5%) to the recovery efficiency. Furthermore, this study demonstrated that the cation load ratio (the ratio between applied current density and cation loading rate) is more suitable than the NH_4-N load ratio for predicting the performance of a (bio)electrochemical membrane-based system for nutrient removal/recovery from complex wastewater streams.

Funding

This work is supported by the Maj and Tor Nessling Foundation [Grant number 201800132]; Tampere University; the KAUTE Foundation [Grant number 20190409]; and the Finnish Foundation for Technology Promotion [Grant number 6602] in support of Veera Koskue. Pablo Ledezma acknowledges a Research Stimulus Fellowship from The University of Queensland.

CRediT authorship contribution statement

Veera Koskue: Conceptualization, Methodology, Investigation, Formal analysis, Visualization, Writing – original draft, Funding acquisition. **Stefano Freguia:** Conceptualization, Methodology, Supervision, Writing – review & editing. **Pablo Ledezma:** Conceptualization, Methodology, Supervision, Writing – review & editing. **Marika Kokko:** Conceptualization, Methodology, Supervision, Writing – review & editing.

Declaration of Competing Interest

The authors declare that they have no known competing financial interests or personal relationships that could have appeared to influence the work reported in this paper.

Acknowledgements

The authors acknowledge the use of the facilities and the scientific and technical assistance provided by the Analytical Services Laboratory at the Advanced Water Management Centre, The University of Queensland

Supplementary material

Supplementary data associated with this article can be found in the online version at doi:10.1016/j.jece.2021.106286.

References

[1] M. Sutton, A. Bleeker, C. Howard, M. Bekunda, B. Grizzetti, W. de Vries, H. van Grinsven, Y. Abrol, T. Adhya, G. Billen, E. Davidson, A. Datta, R. Diaz, J. Erisman, X. Liu, O. Oenema, C. Palm, N. Raghuram, S. Reis, R. Scholz, T. Sims, H. Westhoek, F.S. Zhang, Our nutrient world: the challenge to produce more food and energy with less pollution, Glob. Overv. Nutr. Manag. (2013).
[2] G. Billen, J. Garnier, L. Lassaletta, The nitrogen cascade from agricultural soils to the sea: modelling nitrogen transfers at regional watershed and global scales, Philos. Trans. R. Soc. B 368 (2013), 20130123.
[3] A. Mulder, The quest for sustainable nitrogen removal technologies, Water Sci. Technol. 48 (2003) 67–75.
[4] M. Maurer, P. Schwegler, T.A. Larsen, Nutrients in urine: energetic aspects of removal and recovery, Water Sci. Technol. 48 (2003) 37–46, https://doi.org/10.2166/wst.2003.0011.
[5] X. Wu, O. Modin, Ammonium recovery from reject water combined with hydrogen production in a bioelectrochemical reactor, Bioresour. Technol. 146 (2013) 530–536, https://doi.org/10.1016/j.biortech.2013.07.130.
[6] C. Fux, H. Siegrist, Nitrogen removal from sludge digester liquids by nitrification/denitrification or partial nitritation/anammox: environmental and economical considerations, Water Sci. Technol. 50 (2004) 19–26, https://doi.org/10.2166/wst.2004.0599.
[7] C.H. Guo, V. Stabnikov, V. Ivanov, The removal of nitrogen and phosphorus from reject water of municipal wastewater treatment plant using ferric and nitrate bioreductions, Bioresour. Technol. 101 (2010) 3992–3999, https://doi.org/10.1016/j.biortech.2010.01.039.
[8] Y.V. Nancharaiah, S. Venkata Mohan, P.N.L. Lens, Recent advances in nutrient removal and recovery in biological and bioelectrochemical systems, Bioresour. Technol. 215 (2016) 173–185, https://doi.org/10.1016/j.biortech.2016.03.129.
[9] V. Koskue, J.M. Rinta-kanto, S. Freguia, P. Ledezma, M. Kokko, Optimising nitrogen recovery from reject water in a 3-chamber bioelectroconcentration cell, Sep. Purif. Technol. 264 (2021), 118428, https://doi.org/10.1016/j.seppur.2021.118428.
[10] J. Desloover, A.A. Woldeyohannis, W. Verstraete, N. Boon, K. Rabaey, Electrochemical resource recovery from digestate to prevent ammonia toxicity during anaerobic digestion, Environ. Sci. Technol. 46 (2012) 12209–12216, https://doi.org/10.1021/es3028154.
[11] A.J. Ward, K. Arola, E. Thompson Brewster, C.M. Mehta, D.J. Batstone, Nutrient recovery from wastewater through pilot scale electrodialysis, Water Res. 135 (2018) 57–65, https://doi.org/10.1016/j.watres.2018.02.021.
[12] M. Rodrigues, T.T. De Mattos, T. Sleutels, A. Ter Heijne, H.V.M. Hamelers, C.J. N. Buisman, P. Kuntke, Minimal bipolar membrane cell configuration for scaling up ammonium recovery, ACS Sustain. Chem. Eng. 8 (2020) 17359–17367, https://doi.org/10.1021/acssuschemeng.0c05043.
[13] J. Desloover, J. De Vrieze, M. Van De Vijver, J. Mortelmans, R. Rozendal, K. Rabaey, Electrochemical nutrient recovery enables ammonia toxicity control and biogas desulfurization in anaerobic digestion, Environ. Sci. Technol. 49 (2015) 948–955, https://doi.org/10.1021/es504811a.
[14] P. Ledezma, J. Jermakka, J. Keller, S. Freguia, Recovering nitrogen as a solid without chemical dosing: bio-electroconcentration for recovery of nutrients from urine, Environ. Sci. Technol. Lett. 4 (2017) 119–124, https://doi.org/10.1021/acs.estlett.7b00024.
[15] J. Jermakka, E. Thompson, P. Ledezma, S. Freguia, Electro-concentration for chemical-free nitrogen capture as solid ammonium bicarbonate, Sep. Purif. Technol. 203 (2018) 48–55, https://doi.org/10.1016/j.seppur.2018.04.023.
[16] J. Monetti, P. Ledezma, B. Virdis, S. Freguia, Nutrient recovery by bio-electroconcentration is limited by wastewater conductivity, ACS Omega 4 (2019) 2152–2159, https://doi.org/10.1021/acsomega.8b02737.
[17] B.E. Logan, B. Hamelers, R. Rozendal, U. Schröder, J. Keller, S. Freguia, P. Aelterman, W. Verstraete, K. Rabaey, Microbial fuel cells: methodology and technology, Environ. Sci. Technol. 40 (2006) 5181–5192, https://doi.org/10.1021/es0605016.
[18] P. Kuntke, M. Geleji, H. Bruning, G. Zeeman, H.V.M. Hamelers, C.J.N. Buisman, Effects of ammonium concentration and charge exchange on ammonium recovery from high strength wastewater using a microbial fuel cell, Bioresour. Technol. 102 (2011) 4376–4382, https://doi.org/10.1016/j.biortech.2010.12.085.
[19] M. Rodríguez Arredondo, P. Kuntke, A. ter Heijne, H.V.M. Hamelers, C.J. N. Buisman, Load ratio determines the ammonia recovery and energy input of an electrochemical system, Water Res. 111 (2017) 330–337, https://doi.org/10.1016/j.watres.2016.12.051.
[20] P. Kuntke, T.H.J.A. Sleutels, M. Rodríguez Arredondo, S. Georg, S.G. Barbosa, A. Heijne, (Bio) electrochemical ammonia recovery: progress and perspectives, Appl. Microbiol. Biotechnol. 2 (2018) 3865–3878, https://doi.org/10.1007/s00253-018-8888-6.
[21] H. Guo, P. Yuan, V. Pavlovic, J. Barber, Y. Kim, Ammonium sulfate production from wastewater and low-grade sulfuric acid using bipolar- and cation-exchange membranes, J. Clean. Prod. (2020), 124888, https://doi.org/10.1016/j.jclepro.2020.124888.
[22] X. Wang, X. Zhang, Y. Wang, Y. Du, H. Feng, T. Xu, Simultaneous recovery of ammonium and phosphorus via the integration of electrodialysis with struvite reactor, J. Membr. Sci. 490 (2015) 65–71, https://doi.org/10.1016/j.memsci.2015.04.034.
[23] Finnish Standards Association, SFS-EN 872:2005, Water quality, Determination of suspended solids, Method by Filtration through Glass Fibre Filters, 2005, pp. 1–10.
[24] M. Rodríguez Arredondo, P. Kuntke, A. ter Heijne, C.J.N. Buisman, The concept of load ratio applied to bioelectrochemical systems for ammonia recovery, J. Chem. Technol. Biotechnol. 94 (2019) 2055–2061, https://doi.org/10.1002/jctb.5992.
[25] S. Guštin, R. Marinšek-Logar, Effect of pH, temperature and air flow rate on the continuous ammonia stripping of the anaerobic digestion effluent, Process Saf. Environ. Prot. 89 (2011) 61–66, https://doi.org/10.1016/j.psep.2010.11.001.

[26] P. Kuntke, P. Zamora, M. Saakes, C.J.N. Buisman, H.V.M. Hamelers, Gas-permeable hydrophobic tubular membranes for ammonia recovery in bio-electrochemical systems, Environ. Sci. Water Res. Technol. 2 (2016) 261–265, https://doi.org/10.1039/c5ew00299k.
[27] P. Kuntke, M. Rodrigues, T. Sleutels, M. Saakes, H.V.M. Hamelers, C.J.N. Buisman, Energy-efficient ammonia recovery in an up-scaled hydrogen gas recycling electrochemical system, ACS Sustain. Chem. Eng. 6 (2018) 7638–7644, https://doi.org/10.1021/acssuschemeng.8b00457.
[28] P. Kuntke, M. Rodríguez Arredondo, L. Widyakristi, A. Ter Heijne, T.H.J. A. Sleutels, H.V.M. Hamelers, C.J.N. Buisman, Hydrogen gas recycling for energy efficient ammonia recovery in electrochemical systems, Environ. Sci. Technol. 51 (2017) 3110–3116, https://doi.org/10.1021/acs.est.6b06097.
[29] J. Monetti, M.E. Logrieco, P. Ledezma, B. Virdis, S. Freguia, Effect of flush water on nutrient recovery from urine using bioelectroconcentration, in: Proceedings of the ISMET7, International Society for Microbial Electrochemistry and Technology Global Conference, 2019.
[30] D. Ippersiel, M. Mondor, F. Lamarche, F. Tremblay, J. Dubreuil, L. Masse, Nitrogen potential recovery and concentration of ammonia from swine manure using electrodialysis coupled with air stripping, J. Environ. Manag. 95 (2012) S165–S169, https://doi.org/10.1016/j.jenvman.2011.05.026.
[31] International Labour Organization (ILO), International Chemical Safety Cards Database, 2018. ⟨https://www.ilo.org/dyn/icsc/showcard.listcards3?p_lang=en⟩. (Accessed 16 March 2021).
[32] R. Sander, Compilation of Henry's law constants (version 4.0) for water as solvent, Atmos. Chem. Phys. 15 (2015) 4399–4981, https://doi.org/10.5194/acp-15-4399-2015.
[33] G. Luo, S. Johansson, K. Boe, L. Xie, Q. Zhou, I. Angelidaki, Simultaneous hydrogen utilization and in situ biogas upgrading in an anaerobic reactor, Biotechnol. Bioeng. 109 (2012) 1088–1094, https://doi.org/10.1002/bit.24360.
[34] M. Rodrigues, T. Sleutels, P. Kuntke, D. Hoekstra, A. ter Heijne, C.J.N. Buisman, H. V.M. Hamelers, Exploiting Donnan dialysis to enhance ammonia recovery in an electrochemical system, Chem. Eng. J. 395 (2020), 125143, https://doi.org/10.1016/j.cej.2020.125143.
[35] E. Thompson Brewster, A.J. Ward, C.M. Mehta, J. Radjenovic, D.J. Batstone, Predicting scale formation during electrodialytic nutrient recovery, Water Res. 110 (2017) 202–210, https://doi.org/10.1016/j.watres.2016.11.063.
[36] M. Rodrigues, A. Paradkar, T. Sleutels, A. ter Heijne, C.J.N. Buisman, H.V. M. Hamelers, P. Kuntke, Donnan dialysis for scaling mitigation during electrochemical ammonium recovery from complex wastewater, Water Res. 201 (2021), 117260, https://doi.org/10.1016/j.watres.2021.117260.
[37] Queensland Government, Environmental Authority EPPR00521513, 2020.
[38] F. Fischer, G. Zufferey, M. Sugnaux, M. Happe, Microbial electrolysis cell accelerates phosphate remobilisation from iron phosphate contained in sewage sludge, Environ. Sci. Process. Impacts 17 (2015) 90–97, https://doi.org/10.1039/c4em00536h.
[39] G.T. Daigger, Oxygen and carbon requirements for biological nitrogen removal processes accomplishing nitrification, nitritation, and anammox, Water Environ. Res. 86 (2014) 204–209, https://doi.org/10.2175/106143013×13807328849459.
[40] J. Jermakka, S. Freguia, M. Kokko, P. Ledezma, Electrochemical system for selective oxidation of organics over ammonia in urine, Environ. Sci. Water Res. Technol. 7 (2021) 942–955, https://doi.org/10.1039/D0EW01057J.
[41] M. Asraf-Snir, J. Gilron, Y. Oren, Scaling of cation exchange membranes by gypsum during Donnan exchange and electrodialysis, J. Membr. Sci. 567 (2018) 28–38, https://doi.org/10.1016/j.memsci.2018.08.009.
[42] J. Foley, D. de Haas, K. Hartley, P. Lant, Comprehensive life cycle inventories of alternative wastewater treatment systems, Water Res. 44 (2010) 1654–1666, https://doi.org/10.1016/j.watres.2009.11.031.
[43] S. Lackner, E.M. Gilbert, S.E. Vlaeminck, A. Joss, H. Horn, M.C.M. van Loosdrecht, Full-scale partial nitritation/anammox experiences – an application survey, Water Res. 55 (2014) 292–303, https://doi.org/10.1016/j.watres.2014.02.032.
[44] M. Ali, S. Okabe, Anammox-based technologies for nitrogen removal: advances in process start-up and remaining issues, Chemosphere 141 (2015) 144–153, https://doi.org/10.1016/j.chemosphere.2015.06.094.
[45] H. Liu, S. Cheng, B.E. Logan, Power generation in fed-batch microbial fuel cells as a function of ionic strength, temperature, and reactor configuration, Environ. Sci. Technol. 39 (2005) 5488–5493, https://doi.org/10.1021/es050316c.